2-1-2007

Evolution of close white dwarf binaries

Vayujeet Gokhale
Louisiana State University

Meng Peng Xiao
Louisiana State University

Juhan Frank
Louisiana State University

Recommended Citation

Gokhale, V., Xiao, M., & Frank, J. (2007). Evolution of close white dwarf binaries. *Astrophysical Journal, 655* (2 I), 1010-1024. https://doi.org/10.1086/510119

Draft version September 10, 2018
Preprint typeset using LaTeX style emulateapj v. 6/22/04

EVOLUTION OF CLOSE WHITE DWARF BINARIES

Vayujeet Gokhale, Xiao Meng Peng, Juhan Frank
Department of Physics and Astronomy,
Louisiana State University, Baton Rouge, LA 70803-4001.
gokhale@baton.phys.lsu.edu.

Draft version September 10, 2018

ABSTRACT

We describe the evolution of double degenerate binary systems, consisting of components obeying the zero temperature mass radius relationship for white dwarf stars, from the onset of mass transfer to one of several possible outcomes including merger, tidal disruption of the donor, or survival as a semi-detached AM CVn system. We use a combination of analytic solutions and numerical integrations of the standard orbit-averaged first-order evolution equations, including direct impact accretion and the evolution of the components due to mass exchange. We include also the effects of mass-loss during super-critical (super-Eddington) mass transfer and the tidal and advective exchanges of angular momentum between the binary components. We cover much the same ground as Marsh et al. (2004) with the additional effects of the advective or consequential angular momentum from the donor and its tidal coupling to the orbit which is expected to be stronger than that of the accretor. With the caveat that our formalism does not include an explicit treatment of common envelope phases, our results suggest that a larger fraction of detached double white dwarfs than what has been hitherto assumed, survive the onset of mass transfer, even if this mass transfer is initially unstable and rises to super-Eddington levels. In addition, as a consequence of the tidal coupling, systems that come into contact near the mass transfer instability boundary undergo a phase of oscillation cycles in their orbital period (and other system parameters). Unless the donor star has a finite entropy such that the effective mass-radius relationship deviates significantly from that of a zero temperature white dwarf, we expect our results to be valid. Much of the formalism developed here would also apply to other mass-transferring binaries, and in particular to cataclysmic variables and Algol systems.

Subject headings: accretion, accretion disks — binaries: close — gravitational waves — stars: novae, cataclysmic variables — stars: white dwarfs

1. INTRODUCTION

Binary white dwarfs which are close enough to be driven together by angular momentum losses due to gravitational radiation, and perhaps additional mechanisms, will undergo a phase of mass transfer during which the ultimate fate of the binary is decided. There are many reasons to revisit these dynamical phases of the evolution of double degenerate binaries today. Chief among these is that a survey of the published literature on the subject reveals that many pieces of the puzzle have been explored in different degrees but we still lack a uniform theoretical understanding of the fate of these binaries for all possible mass ratios, orbital parameters and origins. Ideally, one would like our theoretical understanding to be such that given a white dwarf binary of arbitrary masses and compositions at the time that the less massive component gets into contact, one could reconstruct the previous evolutionary pathways and the subsequent evolution to merger, tidal disruption or stable mass transfer.

The reason for this lack of uniformity is that understanding double white dwarf binaries (DWD) in this rapid phase of interaction can be quite complex and demanding, necessitating detailed hydrodynamics, nuclear physics, radiative transfer and stellar structure. Therefore it is natural that different assumptions and techniques are used when one attempts to answer a question relevant to different classes of phenomena. For example, the approaches adopted in studying the putative progenitors of supernovae of type Ia, or the sources of gravitational waves for LISA, or the progenitors of AM CVn binaries, are all very different. While we shall not attempt to cover all the rich physics that may be ultimately necessary to have a uniform and reliable treatment of all possible outcomes of the interaction, we will describe these interactions within a single semi-analytic framework, making connections where appropriate to well-known results already in the literature.

Our particular motive for having developed the understanding described in this paper is that our group has been improving and running a 3-D numerical hydrocode (Motl et al. 2002; D'Souza et al. 2006) which is currently capable of following self-consistently the evolution of model white dwarf binaries through these rapid phases of mass transfer, tracking mass and angular momentum with high accuracy for over 30 orbital periods. In the course of numerous evolutions in which we controlled the rate of driving by angular momentum losses, or prescribed an arbitrary rate of pseudo-thermal expansion of the donor, it became clear that we needed some simpler insight into the behavior of the models. This led us to extend the analytic solution of Webbink & Iben (1987) (WI) for the time-dependent behavior of the mass transfer by relaxing most of the assumptions made to render the problem tractable. Here, we retain the simplifying assumption of Roche geometry, but allow all the binary parameters to vary self-consistently. Thus we investigate numerically a system of first-order evolution equations for a variety of cases and recover the WI

solution when appropriate conditions are applied. We then extend our insight to more general cases, and comment on the applicability and limitations of our approach. While we are still far from the more ambitious goal described above, we think that the present investigation may also provide a useful framework for other workers in the field of binary evolution and especially for those interested in large-scale numerical simulations of these binaries. Many of the techniques and theoretical insights in this paper are applicable to other semi-detached binaries and may have some relevance to contact binaries.

2. BASIC EQUATIONS

Consider a binary having nearly spherical components of masses M_1 and M_2 and separation a. Without loss of generality, we shall assume that as this binary evolves from a detached to a semi-detached state, star 2 is the one that fills its critical Roche lobe and becomes the donor. We define the mass ratio of the binary to be $q = M_2/M_1$. Assuming for simplicity that the spin axes of the individual components of the binary are perpendicular to the orbital plane, and that the orbit is circular, the total angular momentum of the system is given by:

$$\begin{aligned} J_{\rm tot} &= J_{\rm orb} + J_1 + J_2 \\ &= M_1 M_2 \left(Ga/M\right)^{1/2} + k_1 M_1 R_1^2 \, \omega_1 + k_2 M_2 R_2^2 \, \omega_2, \end{aligned} \tag{1}$$

where k_i are dimensionless constants depending on the internal structure of the components and ω_i are the angular spin frequencies. The first term in eq. (1) represents the orbital angular momentum of the components, and the two other terms represent the spin angular momenta of the stars. The form of the orbital angular momentum term adopted above assumes the binary revolves at the Keplerian frequency $\Omega = (GM/a^3)^{1/2}$, which is a good approximation if the stars are centrally condensed.

For a fully synchronous configuration, it is easy to show that the total angular momentum and the total energy have a minimum at the same separation $a_{\rm min} = [3(I_1 + I_2)/\mu]^{1/2}$, where the $I_i = k_i M_i R_i^2$ are the moments of inertia of the components, and μ is the reduced mass. Even if the orbital frequency and the spin frequency are not synchronized but remain proportional to one another ($\omega_i = f_i \Omega$), there is a minimum of $J_{\rm tot}$ at some $a_{\rm min}$. Also the total energy of the system will have a minimum but in general it will not occur at $a_{\rm min}$.*

For our purposes it will be sufficient to work with the approximate form of eq. (1) given above. A more complete and thorough discussion of the secular and dynamical stability of polytropic binaries has been presented in two well-known series of papers by Lai, Rasio & Shapiro (LRS1-LRS5) and further developed with SPH simulations in papers by Rasio & Shapiro (RS1-RS3), who also addressed the role of mass-transfer.

If the donor has a relatively soft equation of state and if $q \neq 1$, the binary tends to become semi-detached and mass-transfer occurs before it falls prey to the tidal instability mentioned above. Mass transfer changes the initial configuration as the system evolves and may either drive the system to smaller separations and thus closer to the onset of the tidal instability or to larger separations and toward stability. Similarly, mass loss from the system can affect the dynamic stability of the system. We investigate the behavior of such systems (in particular DWD binaries) in the cases of conservative and non-conservative mass transfer, driven by gravitational wave radiation (GWR).

2.1. *Orbital and spin angular momentum*

A system of two point masses orbiting around each other, in circular orbits, radiates gravitationally (Landau & Lifshitz 1975). The loss of orbital angular momentum as a result is given by

$$\left(\frac{\dot{J}}{J}\right)_{\rm GWR} = \; -\frac{32}{5}\frac{G^3}{c^5}\frac{M_1 M_2 M}{a^4} \tag{2}$$

Although GWR is likely to be the only important mode of angular momentum loss from DWD binaries, for any general form of systemic angular momentum loss $\dot{J}_{\rm sys}$, we can re-arrange eq. (1) to obtain

$$J_{\rm orb} = J_{\rm tot} - (J_1 + J_2) \Rightarrow \dot{J}_{\rm orb} = \dot{J}_{\rm sys} - (\dot{J}_1 + \dot{J}_2)\,, \tag{3}$$

allowing for the possibility of spin-orbit coupling of the angular momenta. The rate of change of the spin angular momentum of each individual star can be given as the sum of the advected or *consequential* angular momentum transport plus the effect of the tidal torques

$$\dot{J}_1 = \dot{M}_1 j_1 + \dot{J}_{1,\rm tid}\ , \tag{4}$$

$$\dot{J}_2 = \dot{M}_2 j_2 + \dot{J}_{2,\rm tid}\ . \tag{5}$$

The term denoting the advected component from the donor has not been included in previous treatments concerning white dwarf donors (Marsh et al. 2004), but has been discussed in the case of evolved donors (see for example, Pratt & Strittmatter (1976) and Savonije (1978)). For this reason, a few remarks clarifying the meaning of the consequential terms are in order. In the above equations j_1 and j_2 indicate the specific angular momenta of the matter

* LRS2 show that for Riemann-S and Roche-Riemann sequences $\mathrm{d}E = \Omega \mathrm{d}J + \Lambda \mathrm{d}\mathcal{C}$, where Λ is the angular velocity of internal motions and $\mathcal{C}$ is the equatorial circulation. Thus, as a binary evolves driven by gravitational wave radiation, circulation is conserved and the minima of E and J will coincide. However tidal dissipation does not preserve $\mathcal{C}$ and thus in general the minima will *not* coincide in the presence of tidal spin-orbit coupling.

arriving at the accretor and the matter *leaving* the donor respectively. In a conservative system these will refer to the specific angular momentum of the *same* material with respect to the center of mass of each star, but at *different* times. We assume that as the stream leaves the donor there is no back torque that could modify the spin of the donor. Therefore j_2 is entirely determined by the instantaneous conditions at the donor. However, the material traveling in the stream experiences a time varying torque due to the binary that changes j_1 at the expense of the orbital angular momentum alone i.e. not torquing the spins of either component. These are the assumptions underlying the standard calculations of j_1 and the estimates of the circularization radius which go back to Flannery (1975) and Lubow & Shu (1975). We will discuss later what are the appropriate values for j_1 and j_2, and write down just the general expressions here. Substituting eqs. (4) and (5) in eq. (3) and rearranging

$$\dot{J}_{\rm orb} = \dot{J}_{\rm sys} - \left[-\dot{M}_2(j_1 - j_2) + \dot{J}_{1,\rm tid} + \dot{J}_{2,\rm tid}\right] \ , \tag{6}$$

where we have assumed conservative mass transfer. Also, we can write the tidal torque as

$$\dot{J}_{1,\rm tid} = \frac{k_1 M_1 R_1^2}{\tau_{\rm s_1}}(\Omega - \omega_1) \tag{7}$$

$$\dot{J}_{2,\rm tid} = \frac{k_2 M_2 R_2^2}{\tau_{\rm s_2}}(\Omega - \omega_2) \tag{8}$$

where $\tau_{\rm s_1}$ and $\tau_{\rm s_2}$ are the synchronization timescales of the accretor and donor respectively (See Section 6.1). Eq. (6) becomes

$$\dot{J}_{\rm orb} = \dot{J}_{\rm sys} + \dot{M}_2(j_1 - j_2) - \frac{k_1 M_1 R_1^2}{\tau_{\rm s_1}}(\Omega - \omega_1) - \frac{k_2 M_2 R_2^2}{\tau_{\rm s_2}}(\Omega - \omega_2) \tag{9}$$

$$= \dot{J}_{\rm sys} + \frac{\dot{M}_2}{M_2}\left[M_2(j_1 - j_2) + k_1 M_1 R_1^2 \frac{\tau_{M_2}}{\tau_{\rm s_1}}(\Omega - \omega_1) + k_2 M_2 R_2^2 \frac{\tau_{M_2}}{\tau_{\rm s_2}}(\Omega - \omega_2)\right] \tag{10}$$

where $\tau_{M_2} = -M_2/\dot{M}_2$ is the mass transfer time scale. In eq. (10) the tidal torques have been placed inside the brackets although, strictly speaking, they are not consequential. In most cases encountered in cataclysmic variables (CVs) and low-mass X-ray binaries (LMXBs), $\tau_{\rm s_1} \gg \tau_{M_2}$ and $\tau_{\rm s_2} \ll \tau_{M_2}$, and thus usually $\omega_1 \gg \Omega$, while $|(\Omega - \omega_2)/\Omega| \sim \tau_{\rm s_2}/\tau_{M_2}$. However, in double degenerate binaries there is considerable uncertainty about the synchronization timescales, and in numerical simulations of mass transfer τ_{M_2} is orders of magnitude shorter than the typical timescales one encounters in long-term accreting binaries. Therefore we will retain both tidal terms and investigate their effect on dynamical evolutions. Note that our eq. (9) is equivalent to eq. (1) of Marsh et al. (2004), with two extra terms arising from the advective and tidal contributions from the donor.

2.2. *Binary separation*

We now derive the equations for the evolution of the binary separation, the radius of the donor and the Roche lobe radius using the above equations. From the functional form of the orbital angular momentum, we know that for a conservative system

$$\left(\frac{\dot{J}}{J}\right)_{\rm orb} = \frac{\dot{M}_2}{M_2}(1 - q) + \frac{1}{2}\frac{\dot{a}}{a}.$$

Comparing this with eq. (9) and rearranging, we obtain

$$\frac{\dot{a}}{2a} = \frac{\dot{J}_{\rm sys}}{J_{\rm orb}} - \frac{\dot{M}_2}{M_2}\left[1 - q - M_2\frac{j_1 - j_2}{J_{\rm orb}}\right] - \frac{k_1 M_1 R_1^2}{J_{\rm orb}\tau_{\rm s_1}}(\Omega - \omega_1) - \frac{k_2 M_2 R_2^2}{J_{\rm orb}\tau_{\rm s_2}}(\Omega - \omega_2) \tag{11}$$

The sign of the quantity in brackets determines whether mass transfer tends to expand the system and thus oppose the effect of angular momentum losses, or lead to enhanced contraction. The change of sign will generally occur at some mass ratio q_a whose value we discuss below. Symbolically we may write

$$\frac{\dot{a}}{2a} = \frac{\dot{J}_{\rm sys}}{J_{\rm orb}} - \frac{\dot{J}_{1,\rm tid} + \dot{J}_{2,\rm tid}}{J_{\rm orb}} - \frac{\dot{M}_2}{M_2}[q_a - q] \tag{12}$$

$$q_a \equiv 1 - M_2\frac{j_1 - j_2}{J_{\rm orb}}, \tag{13}$$

Thus (remembering that $\dot{M}_2$ is intrinsically negative) if $q > q_a$, mass transfer will contribute to reducing the separation and, as we will see below, tend to make the binary more unstable to mass transfer. On the other hand, if $q < q_a$, mass transfer will oppose the effects of driving and will tend to stabilize the binary. As q decreases on mass transfer, it is possible that a system which started life with $q > q_a$ may evolve to a more stable configuration, if it does not fall prey to the tidal instability. In eq. (12) the tidal synchronization torques may be considered additional contributions to the driving and they may subtract or add angular momentum to the orbit depending on the case. Note that q_a should be interpreted as the mass ratio at which the last term in eq. (12) changes sign. Its value can be estimated from

the initial mass ratio since it is a slowly varying function of q in the conservative case, but in general it is obtained self-consistently as the binary evolution is followed numerically.

The second term in the definition of q_a represents the effects of the net consequential transfer of angular momentum from orbit to spins. We introduce the symbol $\zeta_{\rm c} = M_2(j_1 - j_2)/J_{\rm orb}$ for this term, noting that it stands for the consequential contribution to $-{\rm d}\log J_{\rm orb}/{\rm d}\log M_2$. For direct impact accretion $j_1 = j_{\rm circ}(\approx b_1^2\Omega)$ is the specific angular momentum carried by the stream as it hits the accretor. The approximate value in parenthesis is valid for a synchronous donor and $b_1 = a(0.5 - 0.227\log q)$ is the distance from the center of mass of the accretor to the inner Lagrangian point L_1 (Frank et al. 2002). With the standard definition of circularization radius $r_h = R_{\rm circ}/a$ (Flannery 1975; Lubow & Shu 1975; Verbunt & Rappaport 1988; Marsh et al. 2004), $M_2 j_{\rm circ}/J_{\rm orb} = [(1+q)r_h]^{1/2}$. Note, however, that the tidal coupling of the donor spin to the orbit was neglected by Marsh et al. (2004), and the consequential term proportional to $j_2 \approx R_2^2\omega_2$ was not included either. The precise value of j_2 depends on the details of the flow in the vicinity of L_1 in a non-synchronous donor (See Kruszewski (1963) and Csataryova & Skopal (2005)). For the purposes of this investigation we will simply adopt $j_2 = R_2^2\omega_2$. With these definitions we may write

$$q_a = 1 - \zeta_{\rm c} = 1 - [(1+q)r_h]^{1/2}(1 - \frac{R_2^2\omega_2}{\sqrt{GM_1R_{\rm circ}}}). \tag{14}$$

The net effect of the consequential redistribution of angular momentum in the binary depends on the sign of $\zeta_{\rm c}$. For DWD binaries, $j_1 > j_2$ during the direct impact stage, and this holds even after the onset of disk accretion, when $j_1 = \sqrt{GM_1R_1}$ and $\zeta_{\rm c}$ becomes smaller but remains positive. In cataclysmic variables and low-mass X-ray binaries, the accretion disk returns via tides most of the angular momentum advected by the stream, the donor is almost synchronous, and the tidal coupling of the accretor to the orbit is very weak. However, in this case $R_1 \ll a$ and thus it is more likely that $j_2 > j_1$. While all the additional terms in eqs. (12, 13) are relatively small, yielding $q_a \approx 1$, in some cases $\zeta_{\rm c} < 0$, and thus $q_a \gtrsim 1$ making these systems slightly more stable.

The expression (14) obtained above proves very useful in the interpretation of results of large-scale numerical hydrodynamic simulations of the dynamical evolution of binaries undergoing mass transfer, with and without driving by angular momentum losses (D'Souza et al. 2006)(see also §6.3).

The Roche lobe radius for the donor is accurately given by the formula due to Eggleton (1983)

$$r_{\rm L} \equiv \frac{R_{\rm L}}{a} = \frac{0.49q^{2/3}}{0.6q^{2/3} + \ln(1+q^{1/3})} \tag{15}$$

and so with the notation of Marsh et al. (2004)

$$\frac{\dot{R}_{\rm L}}{R_{\rm L}} = \zeta_{r_{\rm L}}\frac{\dot{M}_2}{M_2} + \frac{\dot{a}}{a},$$

where $\zeta_{r_{\rm L}} \approx 1/3$ is the logarithmic derivative of $r_{\rm L}$ with respect to M_2[†]. Collecting results, we get

$$\frac{\dot{R}_{\rm L}}{R_{\rm L}} = \frac{2\dot{J}_{\rm sys}}{J_{\rm orb}} - 2\frac{\dot{J}_{1,\rm tid} + \dot{J}_{2,\rm tid}}{J_{\rm orb}} - \frac{2\dot{M}_2}{M_2}[q_a - \frac{\zeta_{r_{\rm L}}}{2} - q] \tag{16}$$

Generalizing the meaning of the symbols introduced by Webbink & Iben (1987) to include tidal and consequential terms, we can write the equivalent expressions

$$\frac{\dot{R}_{\rm L}}{R_{\rm L}} = \nu_{\rm L} + \zeta_{\rm L}\frac{\dot{M}_2}{M_2} \tag{17}$$

$$\nu_{\rm L} = \frac{2\dot{J}_{\rm sys}}{J_{\rm orb}} - 2\frac{\dot{J}_{1,\rm tid} + \dot{J}_{2,\rm tid}}{J_{\rm orb}} \tag{18}$$

$$\zeta_{\rm L} = -2q_a + \zeta_{r_{\rm L}} + 2q, \tag{19}$$

where the symbol ν stands for driving terms and the ζ for logarithmic derivatives with respect to donor mass. In the same spirit we write the logarithmic time derivative of the donor radius $R_2 \equiv R_2(M_2, t)$ as:

$$\frac{\dot{R}_2}{R_2} = \nu_2 + \zeta_2\frac{\dot{M}_2}{M_2} \tag{20}$$

where $\nu_2 = (\partial \ln R_2/\partial t)_{M_2}$ represents the rate of change of the donor radius due to intrinsic processes such as thermal relaxation and nuclear evolution, whereas ζ_2 usually describes changes resulting from adiabatic variations of M_2 (D'Antona, Mazzitelli & Ritter 1989). More generally, since the radial variations due to the above mentioned effects operate on different timescales, it is more appropriate to think of ζ_2 as the effective mass-radius exponent, averaged over the characteristic timescale of mass transfer. If the donors are degenerate as in the WD case, or if thermal relaxation is sufficiently rapid, ζ_2 is simply obtained from the equilibrium mass-radius relationship for the donor. But in non-degenerate donors, if the thermal relaxation timescale $\tau_{\rm th}$ becomes comparable to the mass transfer timescale $\tau_{M_2} = M_2/\dot{M}_2$, as is thought to occur during the evolution of CVs, the effects of thermal lag in the donor radius become important, and ζ_2 deviates from the equilibrium value (See Appendix A).

[†] In the range $0 < q \leq 1$, the function $\zeta_{r_{\rm L}}$ takes values between 0.32 and 0.46, and is well approximated by $\zeta_{r_{\rm L}} \approx 0.30 + 0.16q$ for $0.1 \leq q \leq 1$

3. MASS TRANSFER RATE

The following discussion of mass transfer and its stability is rooted in a similar treatment of mass transfer under consequential angular momentum losses (King & Kolb 1995). For all types of donor star, the mass transfer rate is a strong function of the depth of contact, defined here as the amount by which the donor overflows its Roche lobe $\Delta R_2 \equiv R_2 - R_{\rm L}$, suitably normalized. We adopt the following expression valid for most cases of interest:

$$\dot{M}_2 = -\dot{M}_0(M_1, M_2, a) f(\Delta R_2), \tag{21}$$

where $\dot{M}_0$ is a relatively gentle function of binary parameters, while f is a rapidly varying dimensionless function of ΔR_2. For example, for polytropic donors with index n, $f = (\Delta R_2/R_2)^{n+3/2}$ (Paczyński & Sienkiewicz 1972); while for a donor with an atmospheric pressure scale height H, $f = \exp(\Delta R_2/H)$ is appropriate (Ritter 1988). In fact, the exact value of the normalization rate $\dot{M}_0(M_1, M_2, a)$ is not important at all in steady state because the equilibrium rate is determined by the rate of driving: given a particular value of $\dot{M}_0$, the depth of contact will adjust to yield the transfer rate sustainable by the driving. In transient situations, if the mass transfer is varying rapidly, or if the depth of contact becomes large, the normalization becomes relevant.

In principle, Eqs. (7), (8), (12) and (16)-(21) completely specify the system and can be numerically integrated, and we discuss some examples of such evolutions later in §5. However, before proceeding, it is more illuminating to analyze the general implications of eq. (21). Under the assumptions mentioned above

$$\ddot{M}_2 = -\dot{M}_0 \frac{\partial f}{\partial \Delta R_2}\Big(\frac{\dot{R}_2}{R_2} - \frac{\dot{R}_{\rm L}}{R_{\rm L}}\Big), \tag{22}$$

where we have neglected the slower variations of $\dot{M}_0$ with system parameters and we have also assumed that the depth of contact is small $\Delta R_2 << R_2$. Thus the mass transfer rate will be steady whenever the size of the donor varies in step with its Roche lobe. From Eqs. (17)-(20) and (22) we obtain the equilibrium mass transfer rate

$$\Big(\frac{\dot{M}_2}{M_2}\Big)_{\rm eq} = \frac{\nu_{\rm L} - \nu_2}{2(q_{\rm stable} - q)} = \frac{\nu_{\rm L} - \nu_2}{\zeta_2 - \zeta_{\rm L}} \tag{23}$$

where

$$q_{\rm stable} = q_a - \frac{\zeta_{r_{\rm L}}}{2} + \frac{\zeta_2}{2}, \tag{24}$$

is the critical mass ratio for stability of mass transfer. The alternative expression on the r.h.s of eq. (23) thus has the same form as in Webbink & Iben (1987), except that here the driving and consequential terms include the effects of tidal coupling and direct impact accretion. Furthermore, we will allow these terms to vary self-consistently as the evolution proceeds (See §5).

For example, if we assume that the binary is synchronized, the orbit circular, the donor is a polytrope of index $n = 3/2$, and $\nu_2 = 0$ (no thermal or nuclear evolution), then $\zeta_2 \sim -1/3$, $\zeta_{r_{\rm L}} \sim 1/3$, and we get

$$\Big(\frac{\dot{M}_2}{M_2}\Big)_{\rm eq} = \frac{\dot{J}_{\rm sys}/J_{\rm orb}}{2/3 - \zeta_{\rm c} - q}$$

which is the familiar form in the case of direct impact DWD's (Marsh et al. 2004), except that here $\zeta_{\rm c}$ is reduced by the contribution from the donor as given by eq. (14).

The equilibrium mass transfer rate was obtained by demanding that $\ddot{M}_2 = 0$ in eq. (22). In general, if $\dot{M}_2 \neq (\dot{M}_2)_{\rm eq}$, one can rewrite this equation as follows:

$$\ddot{M}_2 = -2\frac{\dot{M}_0}{M_2}\frac{\partial f}{\partial \Delta R_2}(q_{\rm stable} - q)\left[\dot{M}_2 - (\dot{M}_2)_{\rm eq}\right]. \tag{25}$$

The sign of the pre-factor on the r.h.s. is negative if $q < q_{\rm stable}$, thus $\dot{M}_2$ will tend toward the equilibrium value and mass transfer is stable. If $q > q_{\rm stable}$ no attainable equilibrium mass transfer exists and mass transfer is unstable.

4. ANALYTIC SOLUTIONS

Assuming that most of the parameters characterizing the binary and the donor remain constant during (the usually much faster) evolution of the accretion rate, it is possible to obtain analytic solutions for the evolution of the accretion rate itself. In this section we generalize the result of Webbink & Iben (1987) to include donors with an arbitrary polytropic index and with an isothermal atmosphere. These can be later compared to our integrations of the evolution equations in which we allow all binary and donor parameters to vary self-consistently and also with the results of large-scale hydrodynamic simulations (D'Souza et al. 2006).

Assuming that the donor in the binary can be represented by a polytrope, the mass transfer rate is given by a formula derived by Jędrzejec (1969) assuming laminar flow, and quoted by Paczyński & Sienkiewicz (1972)

$$-\dot{M}_2 = \dot{M}_0\Big(\frac{R_2 - R_{\rm L}}{R_2}\Big)^{n+3/2} \tag{26}$$

Raising both sides of the above equation to the power $2/(2n+3)$ and differentiating, we obtain

$$\frac{d}{dt}(-\dot{M}_2)^{2/2n+3} = (\dot{M}_0)^{2/2n+3}[(\nu_2 - \nu_{\rm L}) + \frac{\dot{M}_2}{M_2}(\zeta_2 - \zeta_{\rm L})], \tag{27}$$

where we have set the factor $R_{\rm L}/R_2$ to unity, given that in most situations $\Delta R_2 \ll R_2$. The analytic solutions discussed here assume that the driving rate $\nu_{\rm L}$, the intrinsic radial variation rate ν_2 (which includes the intrinsic thermal and nuclear evolution), and radial reaction exponents $\zeta_2, \zeta_{\rm L}$ remain constant while the depth of contact changes. This is only approximately true; and a self-consistent solution will require numerical integrations. It is interesting first to look at the implications of equation (27) when no driving is present, because the solution is immediate and instructive. This is a situation we encounter in some large-scale hydrodynamic simulations of mass transfer in polytropic binaries (D'Souza et al. 2006). Defining a positive dimensionless mass transfer $y = (-\dot{M}_2/\dot{M}_0)^{2/(2n+3)}$, and a characteristic time scale $\tau = M_2/\dot{M}_0$, eq. (27) becomes

$$\frac{{\rm d}y}{{\rm d}t} = -\frac{\zeta_2 - \zeta_{\rm L}}{\tau} y^{n+3/2}. \tag{28}$$

The solution can be easily inverted to yield

$$y(t) = y(0)\left[1 + y(0)^{n+1/2}(n+1/2)(\zeta_2 - \zeta_{\rm L})t/\tau\right]^{-\frac{2}{2n+1}}, \tag{29}$$

where $y(0)$ is the initial mass transfer rate, normalized as above. This solution illustrates explicitly the role of $\zeta_2 - \zeta_{\rm L} = 2(q_{\rm stable} - q)$. In the stable case, $\zeta_2 > \zeta_{\rm L}$, the mass transfer decays asymptotically to zero over a characteristic time $\tau_{\rm chr} = \tau/[(n+1/2)y(0)^{n+1/2}(\zeta_2 - \zeta_{\rm L})]$, whereas in the unstable case, $\zeta_2 < \zeta_{\rm L}$, it will blow up in finite time equal to $\tau_{\rm chr}$. Thus the essence of the stability of mass transfer in a binary is already contained in the simple case of no driving. The presence of driving exacerbates the natural instability or, in the stable case, the mass transfer settles asymptotically to a non-zero stable value. This is what we observe, for example, in CVs, AM CVns and LMXBs.

Returning now to eq. (27), with the same definitions as above for y and τ, we obtain for the general case in which driving is present,

$$\frac{{\rm d}y}{{\rm d}t} = -\frac{\zeta_2 - \zeta_{\rm L}}{\tau}(y^{n+3/2} - y_{\rm eq}^{n+3/2}), \tag{30}$$

where $y_{\rm eq}^{n+3/2} \equiv -(\dot{M}_2)_{\rm eq}/\dot{M}_0 = (\nu_2 - \nu_{\rm L})\tau/(\zeta_2 - \zeta_{\rm L})$ is the equilibrium value normalized to $\dot{M}_0$. Note that in the stable case, this value is positive; while it is negative in the unstable case. Before we attempt to solve the above differential equation, it is clear from its form and the signs just discussed, that it describes a stable solution in which $y \to y_{\rm eq}$ when $q < q_{\rm stable}$. If, however, $q > q_{\rm stable}$, the r.h.s is positive even if the mass transfer vanishes initially, and it just gets bigger as the mass transfer grows. Since y diverges for the no-driving case in a finite time, the driven case diverges even sooner.

In order to obtain an analytic solution to eq. (27) which can be compared to the solution of Webbink & Iben (1987), it is necessary to cast it in a slightly different form using the equilibrium rate defined in eq. (23), and modifying appropriately the definitions of the integration variable and characteristic time. With the definitions $y_* \equiv [\dot{M}_2/(\dot{M}_2)_{\rm eq}]^{2/(2n+3)}$, and $1/\tau_* \equiv (\nu_2 - \nu_{\rm L})(\dot{M}_2/|(\dot{M}_2)_{\rm eq}|)^{2/(2n+3)}$, the differential equation for the evolution of mass transfer becomes

$$\frac{{\rm d}y_*}{{\rm d}t} = {\rm sgn}(y_*)\frac{1}{\tau_*}(1 - {\rm sgn}(y_*)|y_*|^{n+3/2}), \tag{31}$$

where ${\rm sgn}(y_*)$ is the sign of y_*. Thus, for the stable case $y_* > 0$, while $y_* < 0$ for the unstable case, and τ_* is defined positive. The general analytic solution comprising both the stable and the unstable case can be given in terms of the hypergeometric function, as follows

$$\frac{t}{\tau_*} = y_* {}_2F_1(1, \frac{1}{n+3/2}; 1 + \frac{1}{n+3/2}, {\rm sgn}(y_*)|y_*|^{n+3/2}). \tag{32}$$

While this solution can be easily plotted numerically, it is not possible in general to invert it to obtain $y_*(t)$. In a few cases, simpler analytic forms can be obtained. For example, the case $n = 3/2$ yields the solution of Webbink & Iben (1987), and the case $n = 1/2$ is particularly simple:

$$\begin{array}{lll} y_* = -\tan(t/\tau_*) & y_* < 0 & \text{unstable} \\ y_* = \tanh(t/\tau_*) & y_* > 0 & \text{stable} \end{array} \tag{33}$$

In the case of isothermal atmospheres, the mass transfer rate (Ritter 1988) is given by :

$$\dot{M}_2 = -\dot{M}_0\, e^{(R_2 - R_{\rm L})/H} \tag{34}$$

where, H is the scale height. This form of the mass transfer equation is much simpler to integrate than the one for polytropes considered above. With the same approximations and notation as in the steps leading to eq. (30), and defining $y = -\dot{M}_2/\dot{M}_0 = \exp((R_2 - R_{\rm L})/H)$, we obtain

$$\frac{1}{y}\frac{dy}{dt} = -\frac{\zeta_2 - \zeta_{\rm L}}{\tau}\frac{R_2}{H}(y - y_{\rm eq}). \tag{35}$$

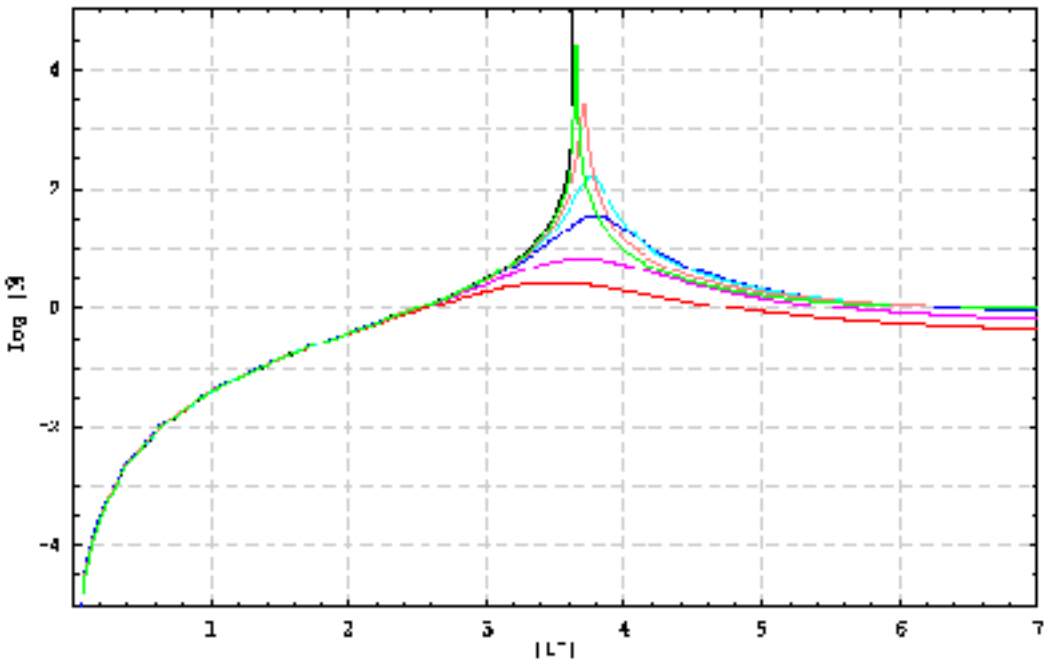

FIG. 1.— Comparison of integrations with the analytic solution by Webbink and Iben. The mass transfer rate normalized to the *initial* equilibrium rate as a function of time in units of the *initial* τ: Analytic (black curve) and numerical – green ($q = 0.663$), orange (0.613), cyan (0.563 same as WI), blue (0.543), magenta (0.523) and red (0.513).

This can be easily integrated to obtain:

$$y = \frac{y_{\rm eq}}{1 - (1 - y_{\rm eq}/y_0)e^{-t/\tau_{\rm iso}}} \tag{36}$$

where $\tau_{\rm iso} \equiv H/R_2(\nu_2 - \nu_{\rm L})$ is the timescale required for the driving to change the depth of contact by $\sim H$, and y_0 is the initial value, always positive for physically meaningful cases. In the stable case $y_{\rm eq} > 0$, and $y \to y_{\rm eq}$, while $y_{\rm eq} < 0$ for the unstable case and y diverges in a finite time $t_{\rm div} = \tau_{\rm iso} \ln(1 - y_{\rm eq}/y_0)$. If no driving is present, we may set $y_{\rm eq} = 0$ and integrate eq. (35) for an isothermal donor. The result is again simple and instructive

$$y = \frac{y_0}{1 + (\zeta_2 - \zeta_{\rm L}) y_0 \frac{R_2}{H} \frac{t}{\tau}} \,. \tag{37}$$

In the stable case, for any initial mass transfer, the system will detach and mass transfer will tend to zero. In the unstable case, any non-zero initial mass transfer will grow and diverge in a finite time.

5. NUMERICAL INTEGRATION RESULTS

We now relax some of the constraints imposed in the previous section and integrate the evolution equations allowing the binary parameters to adjust self-consistently. Specifically, we compute the changes in the masses of the components (assuming conservative mass transfer), allow the binary separation to change as a result of any driving present, and compute the values of ζ_2 and $\zeta_{\rm L}$ as they evolve. The values of ζ_2 depend on the adopted mass-radius relationship for the donor. Here we use Eggleton's interpolated zero-temperature mass-radius relationship cited by Verbunt & Rappaport (1988) and Marsh et al. (2004), which is a good approximation for systems containing old, cold white dwarfs. It is possible that the systems emerge from a common envelope evolution with a massive hydrogen atmosphere around the donor (D'Antona et al. 2006), or that the donor has a finite entropy such that ζ_2 deviates significantly from the value obtained from the zero temperature mass-radius relationship for white dwarfs (Deloye, Bildsten & Nelemans 2005). In such situations, the radial variation rate ν_2 is non-zero, and in fact can reduce the *net driving rate* $\nu_L - \nu_2$, leading to a lower value for the equilibrium mass transfer (see Eq. 23). Also, a mass radius exponent (ζ_2) significantly different from $\approx -1/3$ clearly affects the stability and evolution of the systems at the onset of mass transfer, and can lead to shrinking orbits even if the mass transfer is stable with $\ddot{M}_2 \approx 0$. In our subsequent analysis, where we are concerned about the long term integrations of the OAE, we set $\nu_2 = 0$ and use the zero-temperature mass-radius relationship. We note that for the study of the onset of mass transfer in finite entropy systems like the ones addressed by Deloye, Bildsten & Nelemans (2005) & D'Antona et al. (2006), a more realistic model for the donor is required. In order to calculate $\zeta_{\rm L}$, we need to either assume or determine from other assumptions how the mass and angular momentum are re-distributed in the binary during mass transfer. As we have seen in §3, this depends on the mode of accretion appropriate for the binary considered: does the stream impact the accretor or is an accretion disk present; is the mass transfer sub-Eddington and conservative, or are mass and angular momentum being ejected from the system following super-Eddington mass transfer. For most of the numerical integrations that follow, we use the appropriate

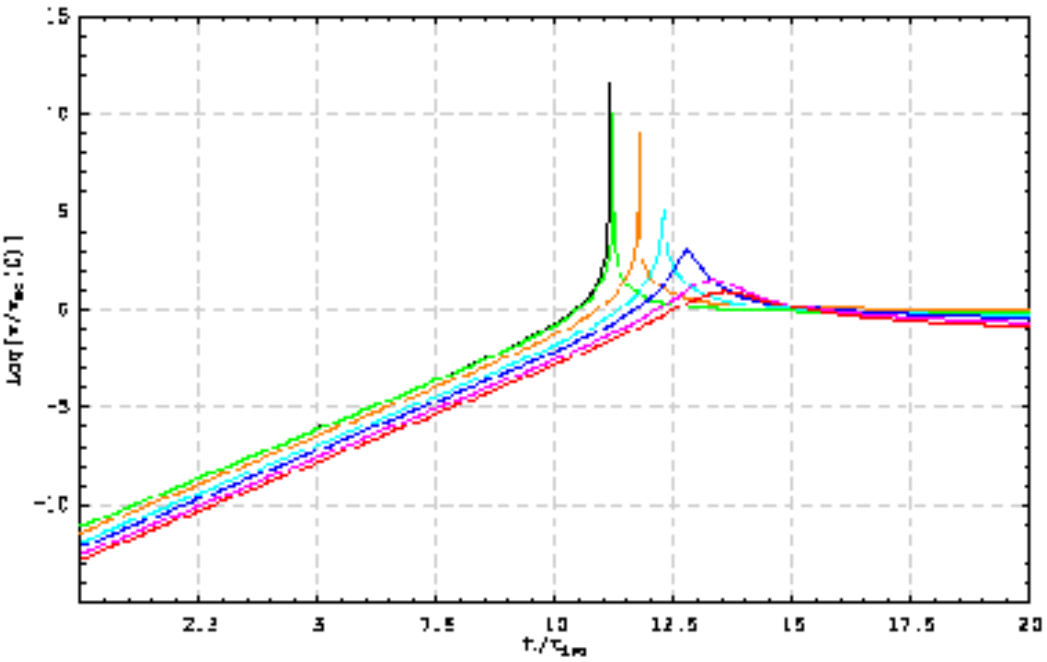

FIG. 2.— Comparison of integrations with the unstable isothermal analytic solution. The natural logarithm of the mass transfer rate normalized to the *initial* equilibrium rate for the case with $q = 0.663$, is shown as a function of time in units of $\tau_{\rm iso}$: Analytic (black curve) and numerical – green ($q = 0.663$), orange (0.613), cyan (0.563 same as WI), blue (0.543), magenta (0.523) and red (0.513).

rate of driving by gravitational wave radiation $\nu_{\rm L}$, wherever necessary we assume a constant driving rate. However, if one is interested in the relatively rapid phases of mass transfer that follow contact and onset, then the qualitative properties of our integrated evolutions do not depend strongly on these assumptions.

5.1. *Surviving unstable mass transfer*

We integrate numerically the evolutionary equations for a sample of double degenerate binaries whose mass ratios at the onset of mass transfer exceed the stable value. In order to mimic the conditions assumed by Webbink & Iben (1987) in their pioneering analysis, we assume a constant rate of driving, that no mass loss from the system occurs even during super-Eddington phases, and that a tidally truncated accretion disk is present at all stages. For these choices, $q_{\rm stable} \approx 0.49$, and thus we expect unstable mass transfer in binaries whose initial mass ratio exceeds this value. In Fig. 1 we present the evolution of mass transfer for a selection of unstable binaries undergoing conservative disk accretion, including the specific value $q = 0.563$ used by Webbink & Iben (hereafter WI) to illustrate their analytic solution. These integrations show that the mass transfer in an initially unstable binary grows at first rapidly, peaks, and then evolves asymptotically toward an equilibrium rate which is also evolving as q changes. The analytic WI solution diverges in a finite time, while all numerical solutions reach a peak and then return to stability. The peak transfer decreases as the initial q approaches $q_{\rm stable}$. The equations we integrate are orbit-averaged evolution equations (OAE) in the sense that the rates of change of the orbital parameters are averaged over one orbital period. This approximation is valid as long as the evolution is not too rapid, and the eccentricity of the orbit remains negligible. Furthermore, our formulation does not include the full effects of tidal distortion and instability discussed by LRS. Our results suggest that an initially unstable binary may survive the onset of unstable mass transfer as long as the mass transfer does not get too big and that the separation does not get too small. See §5.2 for a discussion of the limits of validity of the OAE under unstable mass transfer.

It is also interesting to compare the analytic solution given by eq. (36) for an isothermal donor in the unstable case, with numerical integrations of the OAEs for various initial mass ratios. This comparison is shown in Fig. 2, with the analytic unstable solution plotted as the single divergent black solid line. We elected to plot the natural logarithm of y, which is simply the depth of contact $R_2 - R_{\rm L}$ in units of the pressure scale height H. All the integrations were started from the same initial depth of contact corresponding to an initial mass transfer of 10^{-5} of the reference rate.

5.2. *Super-Eddington mass transfer*

Another effect may come into play as discussed by Han & Webbink (1999) when the mass transfer exceeds the critical Eddington rate and the evolution becomes non-conservative. We can incorporate this effect into our numerical integrations, allowing the excess mass to be blown out of the binary as a wind, carrying away a specific angular momentum $j_{\rm w}$. We calculate the accreted fraction β following Han & Webbink (1999), and modify the evolution equations as follows:

$$\dot{J}_1 = -\beta \dot{M}_2 j_1 + \dot{J}_{1,\rm tid} \ , \tag{38}$$

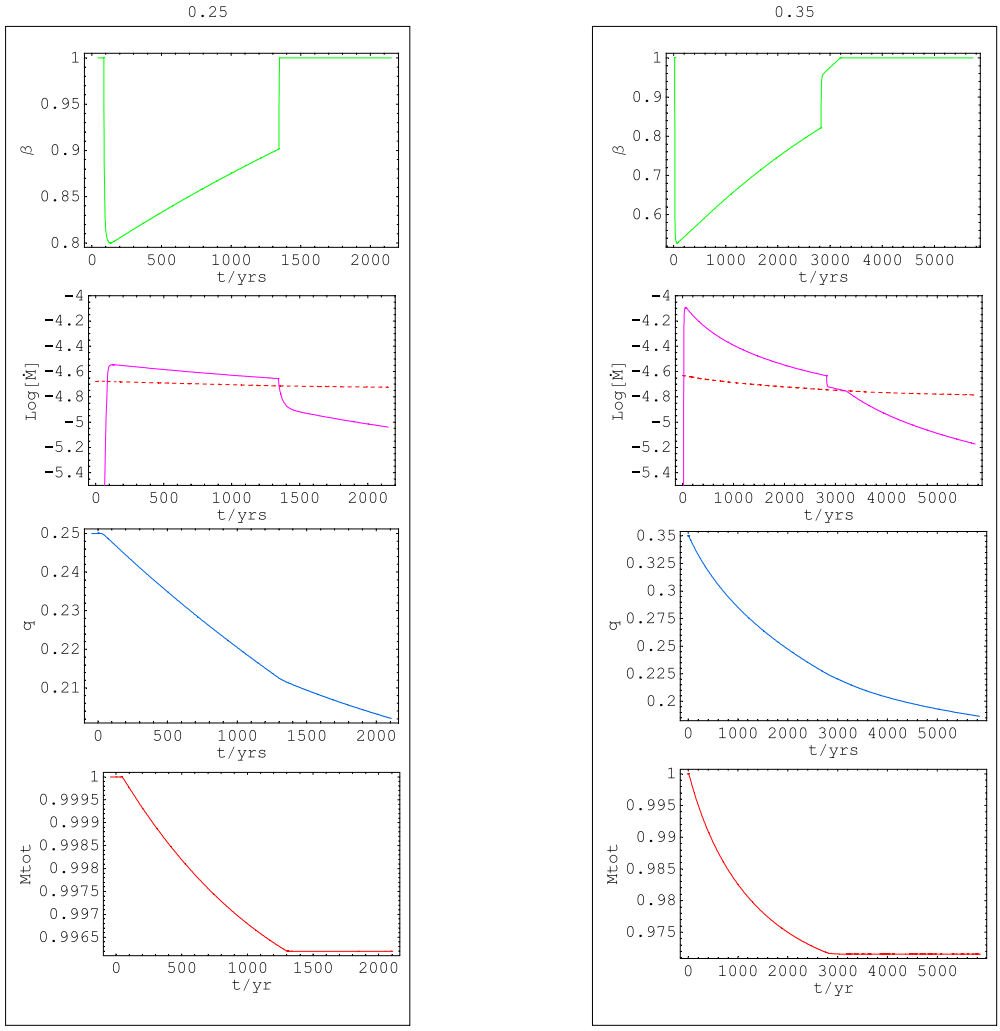

FIG. 3.— Various parameters for super-Eddington accretion with direct impact with $q = 0.25$, just above $q_{\rm stable}$ and $q = 0.35$, well above $q_{\rm stable}$. The panels show from the top down: the accreted fraction β; the logarithm of the mass transfer rate (magenta) and the corresponding Eddington rate (dashed red) in $M_\odot$/yr; the mass ratio q; and the total mass normalized to the initial value. The abscissa shows times in years from the time of first contact. The lower q accretes at super-Eddington rates for less time as compared to the higher q; and it does so more gradually losing less mass (last panel). Even for the initially more unstable mass transfer (larger q), the fraction of mass lost is below 3%.

$$\dot{J}_2 = \dot{M}_2 j_2 + \dot{J}_{2,\rm tid} \ , \tag{39}$$

$$\dot{J}_{\rm orb} = \dot{J}_{\rm sys} - \left(-\dot{M}_2[\beta j_1 - j_2 + (1-\beta) j_{\rm w}] + \dot{J}_{1,\rm tid} + \dot{J}_{2,\rm tid} \right) \ , \tag{40}$$

$$\frac{\dot{a}}{2a} = \frac{\dot{J}_{\rm orb}}{J_{\rm orb}} - \frac{\dot{M}_2}{M_2} \left(1 - \beta q - \frac{1-\beta}{2(1+q)} \right) \ . \tag{41}$$

During the direct impact phase, it is reasonable to assume that the material blown out carries away the characteristic specific angular momentum of the stream $j_{\rm w} = j_1$. After a disk forms, the angular momentum advected by the wind will depend on details of the flow beyond the scope of the present study. For example, if the material is lost mostly from the vicinity of the accretor, it will carry approximately the specific orbital angular momentum of the accretor. Since we do not know exactly how $j_{\rm w}$ varies, we set $j_{\rm w} = j_1$ throughout. In this case eq. (40) simply reduces to eq. (6). While it would be possible to cast the evolution equation for the binary separation (41) in the same form as eq. (12) by defining

$$q_a \equiv 1 + (1-\beta) q - \frac{1-\beta}{2(1+q)} - M_2 \frac{\beta j_1 - j_2 + (1-\beta) j_{\rm w}}{J_{\rm orb}} \ , \tag{42}$$

the explicit appearance of q above makes it obvious that q_a must be calculated self-consistently during the evolution. Note that when $\beta = 1$, the above expression reduces to eq. (13), as it should. Fig. 3 shows two examples of evolutions with a super-Eddington mass-transfer phase. Because the OAE do not include tidal distortions of the components or dissipative effects, arising for example from friction during a common envelope phase, they always predict survival, no matter how high the mass transfer gets during an unstable phase. The only exception to this rule occurs if during

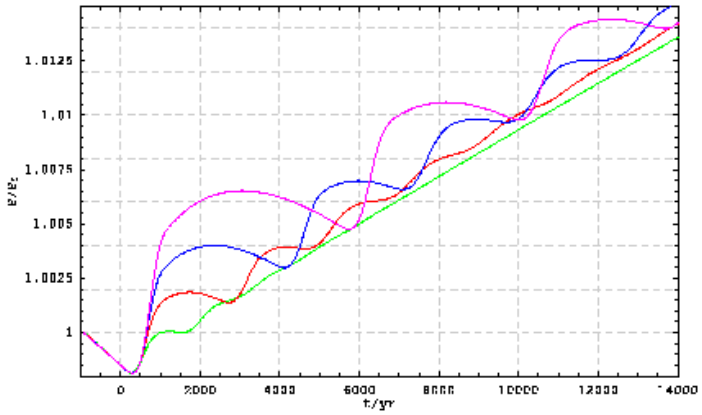

FIG. 4.— Evolution of the period normalized to the period of first contact and onset of mass transfer, for a binary with initial values $q = 0.28$, and $M_2 = 0.125 M_\odot$. This choice yields an orbital period of ≈ 300 s at onset. The curves shown correspond to different *initial* tidal synchronization times; $\tau_{s_1} = 500$ yrs (green), 1000 yrs (red), 1500 yrs (blue) and 2000 yrs (magenta). Tidal timescales are evolved according to eq. (44). The longer the tidal timescale, there are more oscillations with higher amplitude.

the evolution the binary separation falls below the value $a_{\rm min}$ at which the angular momentum and the energy of the binary reach a minimum. In that case, further loss of angular momentum inevitably breaks the synchronism and the system is secularly unstable. As the binary frequency increases, the spin frequencies of the components fall behind, tidal synchronization torques further reduce the orbital angular momentum, and finally a dynamical instability leads to a rapid merger. However, for DWD binaries the lower mass component almost always fills its Roche lobe at a "contact separation" $a_{\rm c}$ well before this minimum is reached. Then mass transfer commences and soon the second term in eq. (11) rises enough to drive the binary apart saving it from a merger. If initially $q > q_{\rm stable}$ mass transfer rises even more quickly and causes the binary to expand and recover from the instability. Clearly the OAE break down if during the transient the transfer is so high that a significant fraction of the donor overflows in one orbit, and the dissipative effects mentioned above may promote a merger even before the mass transfer gets that high.

Suppose that during the transient, the mass transfer rises to ξ times the critical Eddington rate. We can estimate the fraction of the donor mass transferred in a single orbit using the standard assumptions about the donor filling its Roche lobe, and taking for simplicity a mass-radius relationship $R_i \approx 5 \times 10^8 (M_\odot/M_i)^{1/3}$ cm. We find

$$\frac{-\dot{M}_2 P}{M_2} = \frac{P}{\tau} \approx 10^{-9} \xi \left(\frac{M_1}{0.5 M_\odot}\right)^{-1/3} \left(\frac{M_2}{0.1 M_\odot}\right)^{-2} . \quad (43)$$

In most of the parameter space this fraction is so small that we can trust the OAEs to describe approximately the correct behavior within the limits of the physical effects included in their derivation. Looking at Fig. 3 of Han & Webbink (1999), we see that $\xi \lesssim 10$ for most cases with the exception of very rare binaries in which the accretor is already very close to the Chandrasekhar limit. Thus we expect a certain fraction of the binaries that come into contact with $q > q_{\rm stable}$ to survive unstable mass transfer, even if it happens to be super-Eddington. However, to estimate the fraction that actually make it through, one would have to deal with the common envelope phase which is beyond the aims of the present study.

6. APPLICATIONS

In the above sections we have developed the basic framework for investigating the evolution of close DWD systems. By imposing the appropriate constraints on the OAE, we have compared our OAE integrations with analytic solutions illustrating the limitations of the latter. In what follows we investigate the consequences of the OAE when they are applied with all effects included. One immediate consequence of the OAE is the phenomenon of tidally induced oscillations which we describe first. Next, we apply the OAE to a grid of systems with different initial component masses in the $M_2 - M_1$ space and study the evolutionary outcome of each of these systems. Finally, we follow the evolution of a single system in order to achieve a better qualitative understanding of the results obtained for this system using a full 3-D hydro-code.

6.1. *Tidally induced cycles*

As a system gets into contact, the binary separation decreases at first until the mass transfer rate is high enough to reverse the trend in a. In unstable or near unstable cases, during this phase the mass transfer timescale $\tau_{\rm M_2}$ decreases rapidly and becomes shorter than the synchronization timescale of the accretor $\tau_{\rm s_1}$, allowing efficient spin-up and building a large asynchronism. As the separation increases, the mass transfer rate begins to fall and correspondingly $\tau_{\rm M_2}$ increases rapidly (See Fig. 1). The synchronization timescale does not evolve as rapidly as the mass transfer rate and eventually $\tau_{M_2} \gtrsim \tau_{\rm s_1}$. Now the angular momentum stored in the spin of the accretor is efficiently returned to the orbit. If enough asynchronism has been built up in the accretor during the spin-up phase, the additional injection of spin angular momentum to the orbit can cause the separation – and consequently the Roche lobe radius of the donor

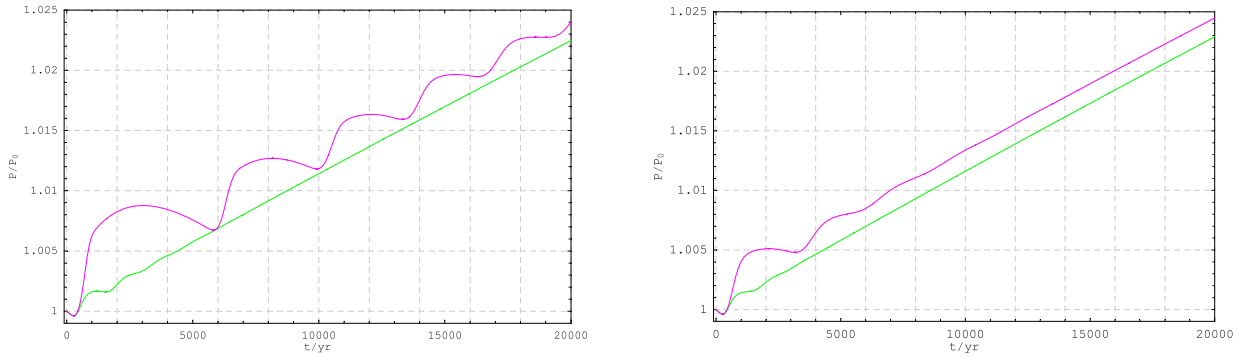

FIG. 5.— *Left Panel*: Evolution of a binary with $q = 0.28$ with $\tau_{s_1} = 2500$ yrs (Magenta) and 500 yrs (Green). *Right Panel*: Same for $q = 0.24$; $\tau_{s_1} = 2500$ yrs (Magenta) and 500 yrs (Green). The time is set to 0 when the binary gets into contact the first time. The higher the mass ratio, the system goes through a larger number of oscillations which are of greater amplitude.

– to increase at a rate faster than the radius of the donor. On the other hand, the donor radius increases at a slower rate due to the decreasing mass transfer rate. This leads to detachment – the radius of the star cannot keep up with the increase in the Roche lobe radius. In general, whenever the effective driving $\nu_L - \nu_2 > 0$, the systems detach. Eventually, when tides synchronize the spins again, the driving will shrink the binary back into contact and accretion recommences, slowly at first, and accelerating as the separation a shrinks and the cycle repeats. However, as the cycles repeat, the deviations from the equilibrium rate decrease until the system settles to a steadily expanding behavior with the mass transfer following the equilibrium rate closely. In the absence of tidal effects, one would expect the orbital period to increase monotonically with time once equilibrium mass transfer has been established for AM CVn type systems. However, in the presence of appropriate tidal coupling, the systems may detach and this leads to oscillations in the orbital period – increasing when the system gets into sufficient contact, and decreasing when it detaches and the GWR dominates over the tidal terms. This behavior is evident from Figs. 4 and 5, in which we plot the orbital period of the binary as a function of time for different mass ratios and tidal synchronization timescales. Notice that the number of oscillations the system goes through is a function of both the tidal timescale and the mass ratio. For a given tidal timescale, the higher the mass ratio, the larger the number of oscillations a system is likely to go through. This is because the higher mass ratio implies that the system is more unstable which leads to a higher mass transfer rate and thus a higher degree of asynchronism between the accretor and the orbit. On the other hand, for a given mass ratio, a longer tidal timescale allows for a higher spin-up of the accretor, leading to more oscillations and higher amplitudes. There are, however, limits to how high or low the tidal timescale (as compared to the mass transfer timescale) can be in order to observe this behavior. If the timescale is too high, the spins and orbit are affectively decoupled whilst if the timescale is too low, the coupling is too efficient to allow for any significant asynchronism. Thus, in these extremes we do not observe any oscillations.

During the evolution of the binary, the tidal synchronization times change because the masses and stellar radii relative to the orbital separation are changing. We assume that the synchronization timescales evolve as in Campbell (1984):

$$\tau_{s_1} \propto \left(\frac{M_1}{M_2}\right)^2 \left(\frac{a}{R_1}\right)^6$$
$$\tau_{s_2} \propto \left(\frac{M_2}{M_1}\right)^2 \left(\frac{a}{R_2}\right)^6 \qquad (44)$$

and choose a normalization (τ_{s_0}) that yields the desired initial timescales. As has been mentioned above, tidally induced detachment has implications for ultra-compact DWD systems ‡; in particular RX J0806 and V407. In these systems it is observed that the orbital period is decreasing at a rate consistent with GWR, but mass transfer is obviously underway in these systems (Strohmayer (2002) and Hakala et al. (2003)). This is at odds with the theoretical expectation that the orbital period should increase. Building on ideas discussed in Lamb & Melia (1987), and complementing cases considered by Marsh & Nelemans (2005), we have investigated the possibility of tidally induced detachment. We see that it is possible for the binary to detach, especially in the case of unstable, direct impact systems. The system parameters like the mass of the donor, accretor and the various angular momentum loss mechanisms are not accurately known for the known AM CVn systems. We have calculated the amount of time the tidal oscillations are in effect in the case of a DWD system after it first gets into contact by loss of GWR for different system parameters. In Table 1 we have tabulated the relevant timescales as a function of the mass ratio q and the tidal timescale τ_{s_1} of the accretor. $T_{osc} = T_1 + T_2 + T_3$ is the timescale for which the oscillations last after initial contact. T_1 represents the time when the binary is in contact but the separation is decreasing, T_2 is the time when the system is in contact and the separation is increasing, whilst T_3 represents the time for which the system is out-of-contact. N_{osc} represents the number of

‡ The higher the donor mass, the shorter the period at initial contact. Also, a higher donor mass makes it more likely that the system has an unstable mass ratio. Thus, in general, oscillations are more likely in short period systems.

TABLE 1
Time spent in different regimes during the oscillation phase as a function of the mass ratio q and tidal timescale τ_{s_1}.

q	τ_{s_1} (yrs)	T_{osc} (yrs)	T_1 (yrs)	T_2 (yrs)	T_3 (yrs)	N_{osc}
0.28	1000	3200	1260	1000	936	1
0.28	2500	23000	4450	4125	14425	4
0.28	5000	64000	4025	11655	48320	5
0.26	1000	0	985	$\forall t > T_1$	0	0
0.26	2500	5400	1750	810	1840	1
0.26	5000	15200	1600	4100	9510	2
0.24	1000	0	710	$\forall t > T_1$	0	0
0.24	2500	3600	1130	1820	650	1
0.24	5000	5500	1110	2300	2100	1

oscillations a system encounters during its evolution. We see that for a given mass ratio, a system tends to spend an increasing amount of time out of contact with increasing tidal timescales. Moreover, the more unstable the mass ratio, the larger the number of oscillations and the timescale for which the oscillations last.

A binary can spend a considerable amount of time in which tides are effective, especially in the case of unstable mass transfer. In fact, since the systems also spend quite a significant fraction of time out-of-contact, there should be many more systems with short periods than can be observed. However, even in the most favorable case, a given system spends less than 30% of its time in a regime where the system is in contact and the orbit is shrinking. Thus it is unlikely that tidally induced oscillations are responsible for the observations of $\dot{P} < 0$ for RX J0806 and V407. Nevertheless, the probability that we catch a system in contact with $\dot{P} < 0$ is enhanced significantly as compared to the case when there are no oscillations (Willems & Kalogera 2005). For example, for the $q = 0.26$ case the system does not undergo any oscillations and $T_1 \sim 1000$ yrs for $\tau_{s_1} = 1000$ yrs. A more promising idea is the recent proposal by D'Antona et al. (2006), according to which the behavior of these systems can be understood if the donor possesses a substantial non-degenerate atmosphere which allows the donor to shrink as mass transfer proceeds. Under these conditions mass transfer tends to be more stable, at least initially, and cycles are unlikely.

In the next section we follow a large number of evolutions with different initial conditions by integrating the OAEs for 10^9 yr, in order to address the question of which kind of systems, and under which conditions, are likely to experience the cycles described here.

6.2. *Exploring Evolutionary Outcomes*

We explore the parameter space for DWD binaries by investigating the different types of binary evolution that can occur under a variety of initial assumptions. Our procedure consists of selecting the initial masses for binary components and evolving them under driving by gravitational radiation for 10^9 yr. In the most general case we include tidal coupling between the orbit and both components, we allow mass loss in super-Eddington cases, and we include the transition from direct impact to disk accretion. We also choose the tidal synchronization timescales for either the accretor alone, as in Marsh et al. (2004) or for both components allowing even the donor to become non-synchronous. As a check, we have evolved a grid of models suppressing the tidal and advective terms from the donor and choosing the same synchronization timescale as Marsh et al. (2004). Under these assumptions our results are indistinguishable from theirs.

Before presenting the results of the evolutions, we investigate the expected behavior of the systems, focussing on the stability limits and whether the mass transfer is super-Eddington or not. In Fig. 6 we plot the stability limits for two cases: one with the donor spin properly accounted for (blue line) and the other with the donor effects ignored (magenta line). In addition for each case, we plot the locus of points for which $\dot{M}_{2_{\rm eq}} \approx \dot{M}_{\rm Edd}$, i.e., the locus of points that defines a transition from super-Eddington accretion to sub-Eddington accretion. Note that these curves represent the equilibrium mass transfer and Eddington rates of the system *at initial contact* where we assume that the systems are synchronous and thus the tidal terms are zero. For direct impact systems the accretion rate is always super-Eddington if $M_2 > 0.21 M_\odot$ (0.17 $M_\odot$ if donor terms are neglected). This is because of two reasons – i) in general, the higher the donor mass, the higher the mass ratio and thus the systems are closer to instability, which in turn implies a higher $\dot{M}_{2_{\rm eq}}$ and ii) the higher the accretor mass, the lower the threshold for super-Eddington accretion (Han & Webbink 1999). However, as can be seen from Fig. 6, the transition of the systems from direct impact to disk leads to changes in the stability properties of these systems – they tend to be slightly more stable because the loss of orbital angular momentum to the accretor spin in disk systems is smaller than in the direct impact case. This is reflected in the slight upturn in the stability curve around $M_1 \sim 1\ M_\odot$ (0.85 $M_\odot$ if donor terms are neglected). The result of this is that the equilibrium mass transfer rate for the disk systems is lower than it would have been for that same system if it were a direct impact system. Consequently these systems tend to undergo sub-Eddington accretion, and the locus of the transition between super and sub-Eddington accretion systems follows the stability curve for both cases. However the disk transition 'saves' only a few systems because DWD binaries with $M_2 > 0.25 M_\odot$, (0.23 $M_\odot$ if

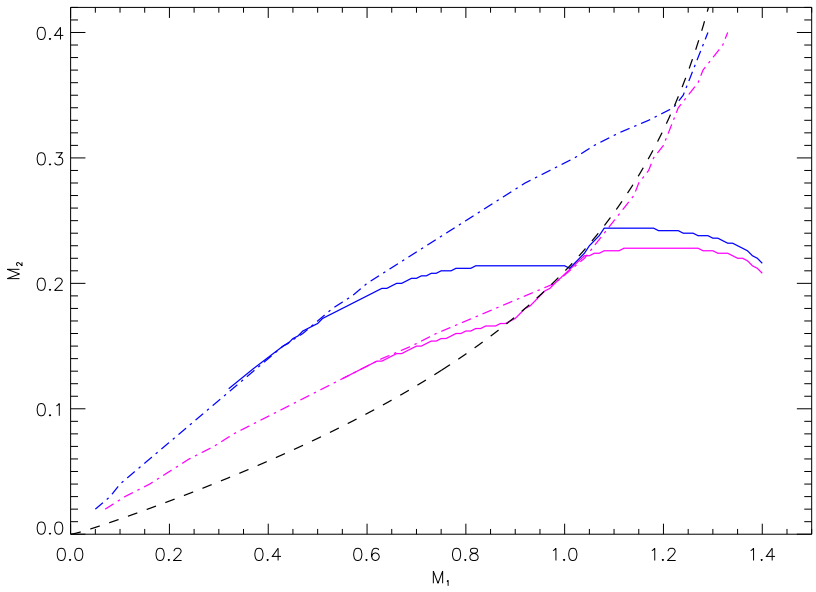

FIG. 6.— Mass-transfer stability limits (dash-dot lines) and super (above) and sub-Eddington (below) accretion boundaries (solid lines) with (blue) and without (magenta) the donor terms included. The thin dashed black line divides direct impact systems from disk accretion systems (Marsh & Steeghs 2002). Because the transition from direct impact to disk accretion makes mass transfer more stable, both the stability limits and Eddington accretion rate boundaries follow closely the locus of that transition toward higher donor masses (see text for details).

donor terms are neglected) are all super-Eddington initially.

We present now the results of the numerical integrations of the OAE for a grid of models in the $M_2 - M_1$ parameter space. In Fig. 7, we plot the results for two extreme values of the accretor tidal synchronization timescales – one with an extremely large tidal timescale (10^{15} yrs) corresponding to inefficient coupling and one for a short timescale of 10 yrs corresponding to highly efficient spin-orbit coupling. Firstly, we note a significantly increased region (as compared to when the donor terms are ignored) of parameter space corresponding to sub-Eddington mass transfer and probable survival as a long-term, stable mass transfer binary of the AM CVn type. Also, from our discussion above, we expect that the case with inefficient tidal coupling (left panel in Fig. 7) to match the curves in Fig. 6. The transition from super to sub-Eddington accretion overlaps the stability boundary until $M_2 \approx 0.21\ M_\odot$ after which it follows the stability curve defined by the direct impact to disk transition, in accordance with our expectations. On the other hand, since the tides almost always act to stabilize the system by effectively reducing the driving rate, a simplistic analysis based on comparing the *initial* equilibrium mass transfer and Eddington rates has only partial validity. While the threshold for super-Eddington accretion remains unaffected by the tidal coupling, the mass transfer rate is significantly lowered due to the reduced driving rate, and can be below the Eddington accretion rate. Systems which have super-Eddington accretion rates when the tidal coupling is inefficient, can thus accrete at sub-Eddington rates if the tidal coupling is strong. As a consequence we expect the domain of sub-Eddington accretion to extend to higher donor masses, and on comparing the left and right panels of Fig. 7 this is what we observe. Finally, the locus of systems that undergo oscillations in their separation and binary period is illustrated in Fig. 8. Whether a system undergoes oscillations or not, depends primarily on two factors: the accretor tidal synchronization timescale τ_{s_1} and the mass ratio q. As can be seen from Fig. 8, oscillations are seen to occur only in a certain domain around the stability curve, and that domain decreases with increasing tidal synchronization times. This is due to the fact that, for higher donor masses, the mass transfer timescale τ_{M_2} is quite short and if the tidal timescale τ_{s_1} is much longer than τ_{M_2}, the spin and the orbit are effectively decoupled. As a result there is minimal return of the spin angular momentum to the orbit and consequently, there are no oscillations for these long timescales. In fact, referring to Fig. 8, we observe that systems with high donor mass ($M_2 > 0.35 M_\odot$) do not undergo any oscillations at all. Again, this is because the mass transfer rates are high in this domain and thus the tidal timescales (considered here) are much longer than the mass transfer timescales. Consequently, the radius of the donor keeps up with the increase in the Roche lobe radius throughout the evolution, and the systems stay in contact.

On the other hand, systems to the bottom right (the ones with low donor mass and high accretor mass) are stable systems and are more likely to be disc-systems. Thus the accretor is not spun up as much as in the case of less stable or unstable systems. Moreover in the disc systems, tides are extremely efficient in returning angular momentum back to the orbit. Both these factors conspire to decrease the level of asynchronism achieved by the accretor and consequently, these systems do not undergo oscillations.

We have also studied the effect of the donor's tidal synchronization timescale on the domain over which systems undergo tidally induced oscillation cycles. In most cases, the level of the donor's asynchronism is rather low. Thus the magnitude of the term associated with the tidal effects of the donor in the driving rate ν_L (eq. (19)) is much smaller

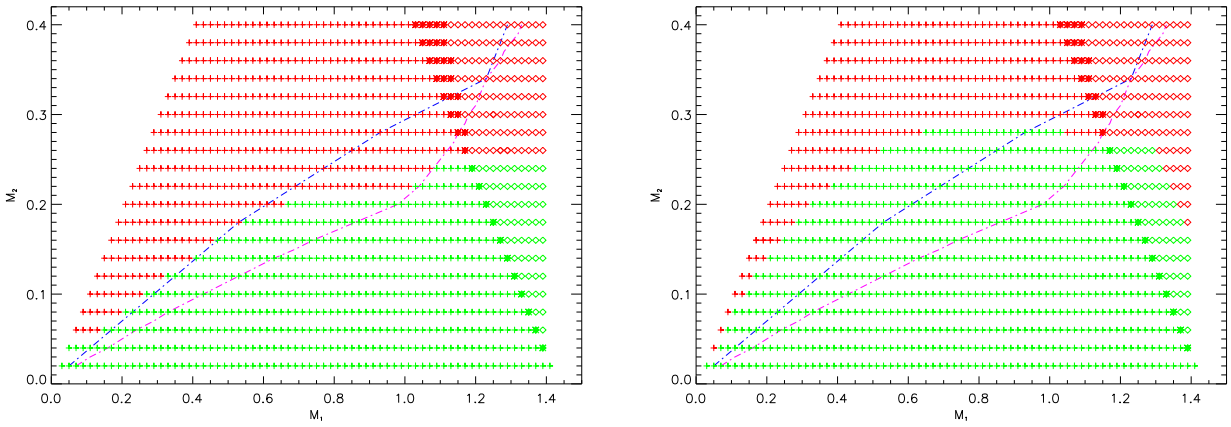

FIG. 7.— Evolution for 10^9 yrs for an initial τ_{s_1} of 10^{15} yrs (left panel) and for τ_{s_1} of 10 yrs (right panel). This synchronization time is for the initial configuration and evolves according to eq. (44). τ_{s_2} is calculated based on whatever τ_{s_0} is required to obtain the desired value of τ_{s_1}. The red symbols represent super-Eddington accretion, the green are sub-Eddington, the pluses (+) and hollow diamonds ($\langle\diamond\rangle$) represent systems with total mass below and above the Chandrasekhar limit, respectively. Among the latter, asterisks over diamonds indicate systems in which the accretor does not reach the Chandrasekhar limit in 10^9 yr. The blue dash-dot line is the initial stability boundary with all donor effects included. The magenta line is the stability boundary without these effects, shown here for comparison. Note the transition in the super and sub-Eddington accretion rate around an M_2 of 0.2 $M_\odot$ to the latter stability curve.

than the corresponding term for the accretor. As a result, the donor synchronization timescale has a limited impact on the domain over which the systems oscillate.

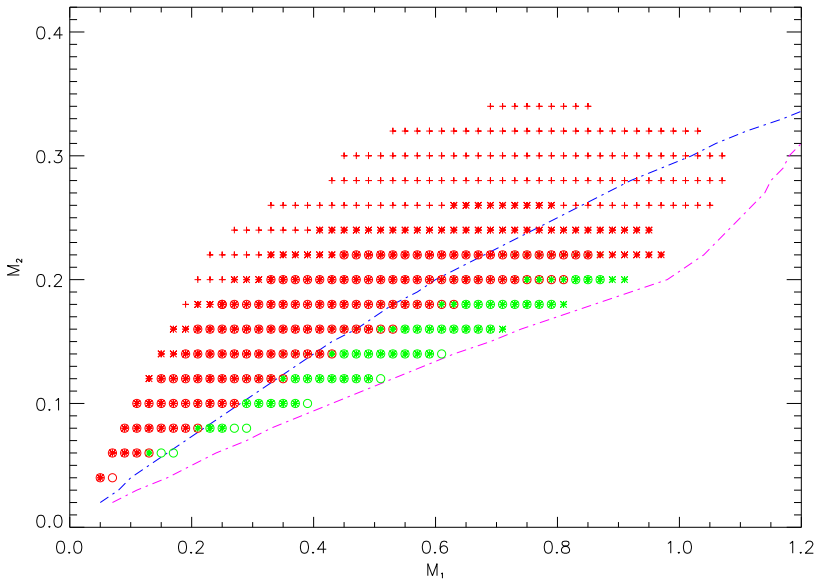

FIG. 8.— Systems which undergo 'oscillations' at least once during their evolution for τ_{s_1} = 500 yrs (pluses, +), 2500 yrs (crosses, ×) and 5000 yrs (open circles, ○). Red indicates super-Eddington transfer during any part of the evolution, whereas green indicates sub-Eddington transfer throughout the 10^9 yr evolution. The magenta and blue lines are the stability limits as in previous figures. τ_{s_2} is held at a constant 100 yrs.

6.3. *Comparison with hydrodynamic simulations*

One of the stated objectives of this paper is to develop a theoretical framework to interpret and analyze results of large-scale, self-consistent, 3-D hydrodynamic simulations of binaries undergoing mass transfer (D'Souza et al. 2006). To this end, we apply the same initial conditions to our OAE as have been to the various runs carried out by D'Souza et al. We have the tidal normalization factor (τ_{s_0}, see eq. (44)) and the mass transfer rate scaling ($\mathfrak{m}$) – such that $\dot{M}_2 = -\mathfrak{m}\dot{M}_0 f(\Delta)$ – as 'free parameters', which we adjust so as to obtain as close a match to the hydro-runs as we can. In the particular run shown in Fig. 9, $\tau_{s_0} = 0.75$ and $\mathfrak{m} = 35.0$. This choice is not unique – indeed, we get reasonable 'fits' even for other combinations of these 'free parameters'. It should be noted that in the numerical simulations of D'Souza et al. (2006) the minimum resolvable mass transfer was on the order of $\sim 10^{-5} M/P$, which translates for short period AM CVn binary parameters to $\sim 10^4 \dot{M}_{\rm Edd}$! Also, in the case of the hydro-runs one observes severe distortion of the accretor and the formation of an accretion belt around the accretor towards the end of the evolution.

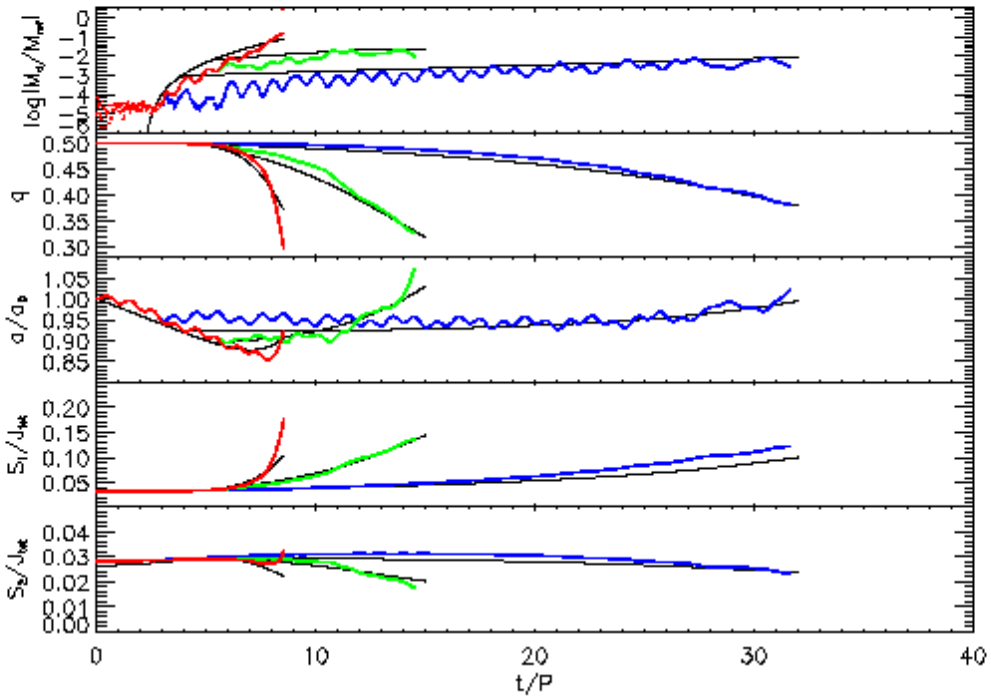

FIG. 9.— Comparison with some of the numerical simulations ($q = 0.5$ run) in D'Souza et al. (2006). Three simulations were performed for the same initial conditions but the binary was driven by angular momentum losses at the level of 1% per orbit for different times in order to achieve increasing depths of contact: Q0.5-a (blue; driven initially for 2.7 orbits), Q0.5-b (green; driven for the first 5.3 orbits) and Q0.5-c (red; driven throughout). The solid black curves show the accretion rate in donor masses per period, the binary mass ratio, the separation normalized to the initial separation, and the spin angular momenta as predicted by the OAEs, while the dotted color curves show the same quantities as derived from the results of the simulations. We arbitrarily change τ_{s_i} of the donor and accretor to match the Q0.5-a run and then predict the outcomes of the other simulations. Here, $\tau_{s_1} \sim 150P$ and $\tau_{s_2} \sim 3.5P$ initially.

These features cannot be easily incorporated in the OAEs, and so the later stages of evolution especially in the case of Q0.5-c, cannot be properly represented in the OAE. An added complication is that for the hydro-runs, the driving was cut off after the systems were thought to have reached a deep enough contact. Since the effective density levels, especially near the edge of the stars in the 3-D numerical model differs from an ideal n = 3/2 polytrope due to the finite numerical resolution of the code, the depth of contact achieved after a certain amount of driving for a certain period of time is not necessarily the same for the hydro-runs and the OAE runs. This is especially true for Q0.5-a, because it is the one which is most sensitive to the depth of contact at the instant the driving is cut-off. For runs Q0.5-b and Q0.5-c, the depth achieved is deep enough to make small differences between the hydro-runs and the OAE unimportant. We are working on another set of runs in which the driving is not cut off and the systems are driven at slightly lower (and more realistic) rates. We hope that this will eliminate another source of discrepancy between the hydro-runs and the OAE.

Despite the above mentioned shortcomings, the OAEs do reproduce reasonably well the behavior of the binaries we have studied. One notices that the hydro-runs have a gentler slope initially which progressively gets steeper as compared to the OAE runs. This, we believe, is a consequence of the complicated fluid flow around the L_1 point and the distortion of the donor star. Moreover, during the initial stages of the evolutions, the 3-D hydrodynamic simulations are subject to numerical noise which is not the case for our numerical integrations. The relative significance of this noise diminishes as the mass transfer rate increases during the evolution. Also, the epicyclic motion that one encounters in the hydro-runs (see D'Souza et al. (2006) for details) cannot be reproduced in our results, since we assume circular orbits. Thus the behavior of the OAE is much smoother than the numerical hydro-runs with no abrupt changes in slopes of the various parameters.

We conclude from the above discussion and Fig. 9, that the OAEs confirm that: a) tidal effects play an important role in the numerical simulations of the binary, b) direct impact accretion is an important effect and can lead to significant spin-up of the accretor at the expense of orbital angular momentum, and c) the OAE prediction that systems that are initially unstable can indeed survive mass transfer seems to bear out in the hydro-runs despite the rather extreme conditions to which the binaries in the hydro-runs are subjected.

In addition to the Q0.5 runs presented above, D'Souza et al. (2006) also present other runs which result in the disruption of the binary. As can be seen from their Fig. 3, 6 and 10, the donor star becomes increasingly distorted towards the end of these simulations. The OAE, at least in their present form, are not capable of accounting for the distortion of the components and the consequence of these distortions on the fate of the binary. Additional hydro-runs with different values of the mass ratio q and lower driving rates ν (though these rates are still orders of magnitude higher than realistic values) are being carried out (Motl, Tohline & Frank 2006). In principle this can help,

for example, in determining a limit on the mass ratio q ($> q_{\rm stable}$) above which the tidal disruption of the binary is likely. However, other physical effects not yet included in the 3-D simulations, such as radiation and the formation of a common envelope, are more likely to determine the fate of such systems.

The tidal time scales that most closely account for the behavior observed in the simulations will serve as a measure of the numerical dissipation present in the simulations. We will present elsewhere a more comprehensive study of the numerical dissipation and its dependence on spatial resolution.

7. DISCUSSION

We have re-examined the standard circular orbit-averaged equations (OAEs) that describe the evolution of mass transferring binaries allowing for advective and tidal exchange of angular momentum between the components. We found that the mass transfer stream issuing through the L_1 point has two effects in the internal redistribution of angular momentum in the binary: 1) it delivers a specific angular momentum $j_{\rm circ}$ to the accretor spinning it up at the expense of the orbital angular momentum; and 2) it reduces the spin angular angular momentum of the donor by a specific amount $\sim R_2^2\omega_2$, and ultimately couples to the orbit via tides. In the cases examined in this paper, the effect of this additional term is mildly stabilizing. For example, with parameters thought to be appropriate for the two short-period, direct impact binaries V407 Vul and RX J0806, the additional donor term is ~ 0.1 (see eq. (24)), so that the net effect of the consequential terms (accretor plus donor) ≈ -0.3, is still de-stabilizing but less than estimated by Marsh et al. (2004), and $q_a \approx 0.7$. Its effect on the evolution of other systems remains to be explored further, but in systems driven by magnetic braking, it is likely to be relatively minor since it is relatively smaller and would be masked by the magnetic torques acting directly on the donor.

We have extended analytically and numerically our understanding of the evolution of stable and unstable mass transfer in semi-detached binaries, with special emphasis on DWD binaries. In particular we have extended the analytic solutions of the type discussed by Webbink & Iben (1987) to other polytropic indexes and the isothermal case. The analytic solutions predict that if $q > q_{\rm stable}$ at contact, the mass transfer rate diverges in a finite time implying the catastrophic merger of the two components. The OAEs on the other hand, always predict that a binary undergoing unstable mass transfer would survive after a phase of rapid mass transfer which in many cases would reach super-Eddington levels. This is because, unlike the analytic case, in the numerical integration of the OAE we allow the binary parameters to evolve self-consistently throughout the evolution. Thus, even if initially $q > q_{\rm stable}$, at some point in the evolution $q < q_{\rm stable}$, and the systems settle to the equilibrium mass transfer rate corresponding to the current values of the system parameters. While we do incorporate mass loss due to super-Eddington accretion, following the treatment along the lines of Han & Webbink (1999), clearly the OAEs must break down if a common envelope forms. The treatment of common envelope evolution is beyond the scope of the present paper, but we suspect that many systems previously considered doomed to a merger would actually survive provided that the mass transfer peak is not too high. This point clearly needs further investigation and probably requires 3-D hydrodynamic simulations with the inclusion of radiative effects.

One interesting consequence of the tidal coupling of the accretor to the orbit is the appearance of mass transfer oscillation cycles occurring for a limited time after the onset of mass transfer. The likelihood of these cycles is higher in situations where the mass transfer is high, or rises to a high value rapidly. Therefore they tend to occur near and around the stability boundaries. Note that all the systems that undergo oscillations are direct impact systems, at least for the system parameters and synchronization timescales we have considered. Thus it is highly unlikely that systems that have accretion disks will undergo the tidally induced oscillation cycles in the case of DWD binaries.

The presence of a massive ($\sim 0.01 M_\odot$) non-degenerate atmosphere on the donor at the onset of mass transfer (D'Antona et al. 2006) can affect the stability and evolution of these systems. For example, a large and positive ζ_2 would imply $q_{\rm stable} > 1$, and has significant implications for cycles, stability boundaries and super-Eddington mass transfer. The full consequences of these circumstances remain to be explored further.

DWD systems are some of the most common compact systems in the galaxy and are of particular importance for the space based gravitational wave detector LISA. AM CVn systems are guaranteed sources for LISA and the knowledge of possible evolutionary trajectories is valuable. The framework we have outlined in this paper can be used to generate templates for short period DWD's in general and AM CVn systems in particular. Similar work has been done already (see for example, Kopparapu & Tohline (2006) and Stroeer et al. (2005)); but the effects of the tidal couplings and the advective term associated with the donor spin remain to be incorporated into future studies.

The LSU theory group has performed a number of large-scale 3-D numerical simulations of interacting binaries with polytropic components (Motl et al. 2002; D'Souza et al. 2006). These simulations did not include enough physics to tackle the common envelope evolution, but they should be viewed as the first steps toward that goal. In the meantime, we have used the OAEs with suitably adjusted tidal coupling time scales to analyze and interpret the results of some of the simulations described by D'Souza et al. (2006). The mass transfer rates that these simulations can resolve are much higher than the Eddington critical rate and probably much higher than the rates likely to arise during the onset of mass transfer in most realistic cases. Nevertheless they describe correctly the dynamical aspects of the mass transfer and tidal interactions under these conditions. Comparing the predictions of the OAEs with the simulations, we were pleased to find that they predict the outcome of the simulations reasonably well.

This work has been supported in part by NASA's ATP program grants NAG5-8497 and NAG5-13430. We thank Joel E. Tohline, Patrick M. Motl and Ravi Kopparapu for helpful discussions. Finally, we would like to acknowledge

the referee for constructive comments.

APPENDIX

THE EFFECTIVE MASS-RADIUS EXPONENT ζ_2

We derive here a simple analytic approximation to the effective mass-radius exponent when the response of the donor is a combination of the adiabatic and thermal adjustments to mass loss. Our starting point is the same as in §3 of D'Antona, Mazzitelli & Ritter (1989), namely

$$\frac{\mathrm{d}\ln R_2}{\mathrm{d}t} = \left(\frac{\partial \ln R_2}{\partial t}\right)_{\rm th} + \left(\frac{\partial \ln R_2}{\partial t}\right)_{\rm nuc} + \zeta_s \frac{\dot{M}_2}{M_2}\,, \tag{A1}$$

where the first two terms on the r.h.s. represent the effects of thermal relaxation and nuclear evolution, and ζ_s is the purely adiabatic mass-radius exponent. The thermal relaxation term may arise as a result of initial conditions, nuclear evolution and mass transfer, and it is usually not possible to disentangle these effects if they operate on similar timescales. However, an approximate description of the radial evolution can be obtained by viewing it as the result of the superposition of thermal relaxation of initial conditions and nuclear evolution, plus a thermal adjustment to mass loss, as follows

$$\frac{\mathrm{d}\ln R_2}{\mathrm{d}t} = \nu_2 + \nu_2' + \zeta_s \frac{\dot{M}_2}{M_2}\,, \tag{A2}$$

where ν_2 is the superposition of intrinsic thermal and nuclear evolution, while ν_2' stands for the rate of thermal radial reaction to mass loss. Our goal is to combine the last two terms on the r.h.s. by absorbing the thermal adjustment to mass loss into an effective mass-radius exponent. We write

$$\zeta_2 \frac{\dot{M}_2}{M_2} = \nu_2' + \zeta_s \frac{\dot{M}_2}{M_2} \tag{A3}$$

where ζ_2 is the effective mass-radius exponent we seek. With the above interpretation, the term ν_2 in eq. (20) represents intrinsic thermal and nuclear processes which may operate on timescales that differ from the standard thermal relaxation rate. This approach is consistent only if $\nu_2 << \zeta_2(\dot{M}_2/M_2)$. Therefore, in what follows, we shall only consider thermal relaxation in response to mass loss, and set $\nu_2 = 0$. As a consequence of the mass loss, the donor's radius R_2 will differ from the equilibrium radius corresponding to its instantaneous mass $R_{\rm eq}(M_2)$. With these definitions we write

$$\frac{\dot{R}_2}{R_2} = \frac{R_{\rm eq}(M_2) - R_2}{R_2 \tau'} + \zeta_s \frac{\dot{M}_2}{M_2} \tag{A4}$$

where we have adopted a simple linear approximation for the thermal reaction term and τ' is the corresponding timescale. The secular evolution of the binary takes place on a mass-transfer timescale $\tau_{M_2} = -M_2/\dot{M}_2$. Differentiating eq. (A4) with respect to time, we get

$$\frac{\mathrm{d}^2\ln R_2}{\mathrm{d}t^2} = \frac{1}{\tau'}\frac{R_{\rm eq}}{R_2}\left(\frac{\zeta_{\rm eq}}{\tau_{M_2}} - \frac{\zeta_2}{\tau_{M_2}}\right) - \frac{\zeta_s}{\tau_{M_2}^2} \tag{A5}$$

If the effective mass-radius exponent is to have any meaning, it must not change much over the evolutionary phase one is considering. Thus, we require

$$\frac{\mathrm{d}^2\ln R_2}{\mathrm{d}t^2} = -\zeta_2/\tau_{M_2}^2\,. \tag{A6}$$

Finally, setting $R_{\rm eq} = R_2$ in eq. (A5), and solving for ζ_2, we obtain

$$\zeta_2 = \frac{\zeta_{\rm eq} + \zeta_s \tau'/\tau_{M_2}}{1 + \tau'/\tau_{M_2}}. \tag{A7}$$

This expression shows that if the evolution is much slower than the thermal relaxation ($\tau' \ll \tau_{M_2}$), the donor radius follows the equilibrium radius closely, whereas if mass transfer occurs rapidly, the donor reacts adiabatically. The above discussion may be applied to cataclysmic variables to describe approximately how the donor becomes increasingly oversized as the orbital period decreases because $\nu_2 \approx 0$. If relaxation from initial conditions or significant nuclear evolution is taking place on timescales comparable to either τ' or τ_{M_2}, the above discussion is strictly not valid.

REFERENCES

Campbell, C.G. 1984, MNRAS, 207, 433

Csataryova, M. & Skopal, A. 2005, Contrib. Astron. Obs. Skalnate Pleso, 35, 17

D'Antona, F., Ventura,P., Burderi, L. & Teodorescu, A., 2006, preprint (astro-ph/0606577)

D'Antona, F., Mazzitelli, I. & Ritter, H. 1989, A&A, 225, 391

Deloye, C., Bildsten, L. & Nelemans, G. 2005, ApJ, 624, 934

D'Souza, M.C., Motl, P.M., Tohline, J.E. & Frank, J. 2006, ApJ, 643, 381

Eggleton, P. P. 1983, ApJ, 268, 368

Flannery, B. 1975, MNRAS, 170, 325

Frank, J., King, A. R., & Raine, D. J. 2002, Accretion Power in Astrophysics (3d ed; Cambridge: Cambridge Univ. Press)
Hakala, P. and Ramsay, G. and Wu, K. and Hjalmarsdotter, L. and Järvinen, S. and Järvinen, A. and Cropper, M., 2003, MNRAS, 343, L10-L14
Han, Z. & Webbink, R.F. 1999, A&A, 349, L17
Jędrzejec, E. 1969, MS thesis, Warsaw University
King, A.R. & Kolb, U. 1995, ApJ, 439, 330
Kopparapu, R. & Tohline J.E., 2006, in preparation
Kruszewski, A. 1963, Acta Astr., 13, 106
Lai, D., Rasio, F.A., & Shapiro, S.L. 1993, ApJ, 406, 63
Lai, D., Rasio, F.A., & Shapiro, S.L. 1993, ApJS, 88, 205
Lai, D., Rasio, F.A., & Shapiro, S.L. 1993, ApJ, 420, 811
Lai, D., Rasio, F.A., & Shapiro, S.L. 1993, ApJ, 423, 344
Lai, D., Rasio, F.A., & Shapiro, S.L. 1993, ApJ, 437, 742
Lamb, D.Q. & Melia, F. 1987, ApJ, 321, L133
Landau, L.D. & Lifshitz, E.M. 1975, The Classical Theory of Fields, Pergamon Press, Oxford
Lubow, S.H. & Shu, F.H. 1975, ApJ, 198, 383
Marsh, T.R. & Steeghs, D. 2002, MNRAS, 331, L7
Marsh, T.R., Nelemans, G. & Steeghs, D. 2004, MNRAS, 350, 113
Marsh, T.R. & Nelemans, G. 2005, MNRAS, 363, 581
Motl, P. M., Tohline, J. E. & Frank, J. 2002, ApJS, 138, 121 (MTF)
Motl, P., Tohline, J. & Frank, J., 2006, *In preparation*
Paczyński B. & Sienkiewicz R.,1972, Acta Astr., 22, 73.
Pratt, J.P. & Strittmatter, P.A., 1976, ApJ, 204, L29
Rasio, F. A. & Shapiro, S. L. 1992, ApJ, 401, 226 (RS92)
Rasio, F. A. & Shapiro, S. L. 1994, ApJ, 432, 242 (RS94)
Rasio, F. A. & Shapiro, S. L. 1995, ApJ, 438, 887 (RS95)
Ritter H., 1988, A&A, 202, 93
Savonije, G.J., 1978, A&A, 62, 317
Stroeer A., Vecchio, A. & Nelemans G. 2005, ApJ, 633, L33
Strohmayer, T.E. 2002, ApJ, 581, 577
Verbunt, F. & Rappaport, S. 1988, ApJ, 332, 193
Webbink, R.F., & Iben, I., Jr. 1987, Proceedings of the 2nd Conference on Faint Blue Stars, p. 445
Willems, B. & Kalogera, V. 2005, preprint (astro-ph/0508218)